

Extreme climate change and contemporary analogs for cities in mainland China in a 2.0 °C warmer climate

Qianzhi Wang^{a,b}, Kai Liu^{a,c,*}, Xiaoyong Ni^d, Ming Wang^a

^a School of National Safety and Emergency Management, Beijing Normal University, China

^b School of Systems Science, Beijing Normal University, China

^c Collaborative Innovation Center on Forecast and Evaluation of Meteorological Disasters (CICFEMD), Nanjing University of Information Science & Technology, China

^d School of National Safety and Emergency Management, Beijing Normal University at Zhuhai, Zhuhai 519087, China

HIGHLIGHTS

- Extreme heat and extreme precipitation changes under 2.0 °C global warming in Chinese cities are quantified.
- Translate the abstract global warming projections into impact assessments that are visible to the public and city managers.
- ~65 % of cities would becoming hotter and all cities would face more extreme precipitation under 2.0 °C global warming.
- Super-large cities in China face stronger changes in extreme heat and extreme precipitation.

ARTICLE INFO

Keywords:

Extreme climate change
City climate analogs
2.0°C global warming

ABSTRACT

Climate change is bringing more extreme weather events, which disrupt the normal functioning of cities and threaten people's lives. The public and city managers need to know the potential change that their cities would experience to better adapt it for sustainable development, which requires better communication of climate information to non-professionals. This study quantified the changes in extreme heat and extreme precipitation in 369 cities in mainland China under 2.0 °C global warming, and a climate-analog mapping was used to visualize the expected climate state in the future of a specific city would be similar to which city's contemporary state. Our results show that 17 % of cities would reach new extreme heat states, and 65 % of cities are becoming hotter. For extreme precipitation, 64 % of northern cities would move southward by an average of 530 km, and 21 % of southern cities would join the contemporary extreme precipitation zones. Specifically, super-large cities with populations larger than 5 million would experience more intense changes, with an average 10 %-40 % greater increases in extreme heat and extreme precipitation than that of all cities. Under significant challenges, identifying similar contemporary cities and learning from their experiences can help managers and public make better preparations to better adapt to changes in extreme weather states.

Practical Implications

- A growing body of warnings and studies has revealed that climate change would bring significant changes in the climate states of cities. On this basis, we focused on the extreme climate change that cities will face in the future. As these cities are often accompanied by cascading and systematic characteristics, extreme climate change will bring severe negative social impacts. We found that both extreme heat and extreme

precipitation would increase in most cities of mainland China and adaptations measures are required to reduce the city risk. Different from the previous papers that tell us the magnitude of precipitation or temperature cities will face, this paper focuses more on translating complex climate projection information into intuitive information that is easier to understand, especially for non-professionals. The extreme climate analogy maps can be used to find out the twin city for extreme heat and precipitation which are of great value for a broad range of users. Specifically, the role is reflected in the following two aspects, (1) Promote public awareness of extreme climate change. Due to the direct

* Corresponding author at: School of National Safety and Emergency Management, Beijing Normal University, #19 Xijiekou Wai Ave., Beijing 100875, China.
E-mail address: liukai@bnu.edu.cn (K. Liu).

link to disasters, extreme weather often makes a stronger impression on the public. When connecting residents' perception of future climate extremes in the city they live in with another contemporary urban state, the exchange of experiences between the residents of the two cities can improve their original abstraction of climate change and a sense of psychological remoteness. (2) Facilitate design of city adaptation measures. Under the similar government structure in China, it becomes easier to transfer the knowledge and management experience of contemporary analogs. For example, city managers can investigate how their contemporary analog adapt to extreme heat and extreme precipitation. It might be installing green and blue infrastructure to make public spaces cooler (Liu et al., 2021), and increasing the proportion of indoor cooling to protect more homes from heat-related illness or death. Preparations for extreme precipitation may be the construction of sponge cities (Chan et al., 2018), which can improve the situation of drainage pipes that have to be heavily relied on due to continuous impervious pavement in traditional urban construction. About 30 cities in China have started pilot programs (Jiang et al., 2018), which can provide a guide to policies, incentives and effects for cities that similar to them. In light of the increasing climate extremes, preparing for the future climate extremes change requires a concerted effort from all sides, and the extreme climate analogy map has the potential to play a role in climate services as a communication tool.

Data availability

Data will be made available on request.

Introduction

Sustainable urban development is one of the important goals of Sustainable Development Goals (SDGs), which aims to make cities and human settlements inclusive, safe, resilient, and sustainable (Vaidya and Chatterji, 2020). Disaster risk reduction is a necessary target, as 59 % of global cities with more than 500,000 inhabitants were at risk of at least one type of disaster (i.e., cyclones, floods, droughts, earthquakes, landslides, and volcanic eruptions) (U.N. Population Division, 2018). Moreover, new evidence strengthens the conclusion that small increments in global warming ($+0.5^{\circ}\text{C}$) can lead to statistically significant changes in extremes for large regions (Seneviratne et al., 2021), and disaster risks in many cities are expected to increase under climate change (Greene et al., 2011; Guerreiro et al., 2018). As populations and assets are highly concentrated in cities, the cost is huge (Bell et al., 2018; Carter et al., 2015; Gao et al., 2015). For example, a record-breaking rainstorm in Zhengzhou, China on July 20, 2021, caused 352 deaths/missing, 114.27 billion yuan of direct economic losses, extraordinary traffic paralysis, 30,616 family homes collapsed, and 0.25 million hectares of crops demolished (People's Government of Henan, 2021). The record-breaking heatwave occurred in the summer of 2022, especially in Europe. In Spain and Portugal, over 2,000 people have died from heat-related causes over roughly a week (Axios, 2022). It is therefore necessary to prepare for and adapt to possible future extreme events to reduce disaster losses and the probability of city paralysis. To achieve this target, the public action (Cheung and Feldman, 2019) and effective decisions by city managers are both required for the sustainable urban development (Casto, 2014).

According to the sixth assessment report of Intergovernmental Panel on Climate Change (IPCC AR6), although more cities around the world have developed adaptation plans since IPCC AR5, few cities have implemented them. The policy-action gap arises from lack of confidence and political inertia when communication is poor, that is, when people cannot foresee the future benefits of adaptation measures (Dodman et al., 2022). Thus, visualizing future scenarios is a useful tool to help

non-professionals from all walks of life anticipate future benefits. Climate-analog mapping is a powerful way to visualize climate change, which can provide the public and city managers with more intuitive concepts (Glantz, 2019). It has been used to improve public awareness, engineering protection, and agricultural adaptation (Hallegatte et al., 2007; Kopf et al., 2008; Mahony et al., 2017; Murawski, 1993; Sanderson et al., 2016; Szenteleki et al., 2012). Webb et al. (2013) compared the temperature and precipitation changes in 23 winegrowing regions worldwide, and it was expected that these regions need to change their cultivars. Bastin et al. (2019) combined 19 bioclimatic variables and three climate models to find climate analogies for global 520 major cities. The results showed that all cities tended to transition to sub-tropical regions, and 22 % of cities will experience new climate states. Fitzpatrick and Dunn (2019) combined the highest seasonal temperatures, lowest seasonal temperatures, and total precipitation and used the improved Mahalanobis distance method to find climate analogs for 540 urban areas in North America. It is estimated that only 17 % of these cities would have similar contemporary cities in the 2080 s under the RCP8.5 emission scenario.

China is a disaster-prone country with a large population and is sensitive to climate change (Byers et al., 2018; Shen and Hwang, 2019). Although climate analogs for some Chinese cities can be found in relevant studies at the global level, to the best of the authors' knowledge, there is a lack of comprehensive studies on future extreme climate analogs for cities in China. For city managers who have similar institutional settings and responsibilities in China, their similar management experience is more valuable. In this study, we used two basic extreme climate indicators, the annual heat days and maximum daily precipitation, to quantify the changes in extreme heat and extreme precipitation in 369 cities in mainland China under 2.0°C global warming. Then, the climate-analog mapping method was used to find the contemporary extreme climate analogs for each city. We further analyzed the changes in super-large cities with more than 5 million people. Finally, the uncertainty of climate models was assessed. Our results provided a scientific basis for urban departments to design long-term climate change adaptation measures to extreme heat and extreme precipitation.

Materials and methods

City definitions

According to the division of administrative regions in China, a total of 369 cities were included in this study. Urban areas were used as the input boundary for each city, as most humans reside in and assets are highly concentrated in. The urban areas were extracted based on land use data (European Space Agency, 2020), and the city administrative boundaries were used to further define them. To facilitate the description of the results, we placed all cities into seven regions based on their geographical locations, as shown in Fig. 1. Super-large cities were chosen for further case analysis. Super-large city refers to the city with a population of more than 5 million, which is consistent with definition of "supercities and megacities" used by Chinese authority, that is, a supercity has a permanent population of 5–10 million, and a megacity has a permanent population of more than 10 million (China State Council, 2014). The WorldPOP data was used here to calculate the population for each urban area, which provided the consistent 1 km resolution population count. For more details, see <https://www.worldpop.org/project/categories?id=3>.

Climate data

The climate data were obtained from NASA Earth Exchange Global Daily Downscaled Projections (NEX-GDDP), which is based on 21 general circulation models (GCMs) from Coupled Model Intercomparison Project Phase 5 (CMIP5) (available online at <https://www.nccs.nasa.gov/services/data-collections/land-based-products/nex-gddp>). Bias-

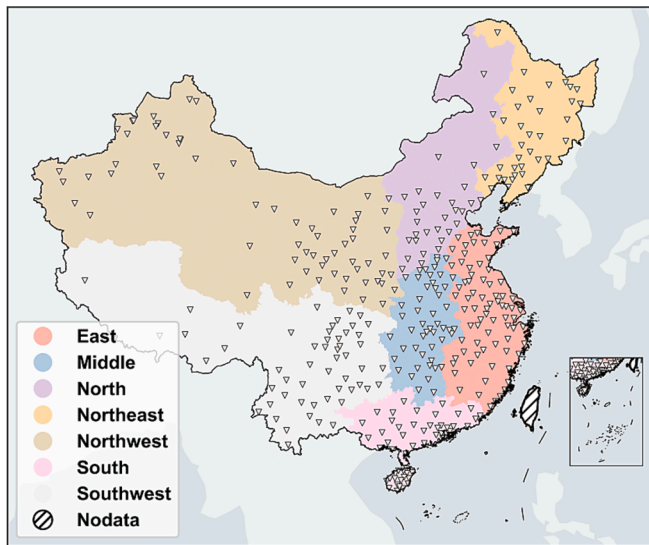


Fig. 1. The locations of cities and their geographical regions in this study (white triangles represent the centroids of urban areas).

correction Spatial Disaggregation (BCSD) method is used to downscale Global Climate Models (GCMs) dataset to a global spatial resolution of $0.25^\circ \times 0.25^\circ$. BCSD is a method specifically developed to address the primary limitations of GCM outputs, i.e., the poor ability of coarse resolution data to capture regional or local climate details and the local bias in the statistical characteristics (Wood et al. 2002; Wood et al. 2004; Maurer and Hidalgo, 2008; Thrasher et al. 2012). Compared with GCMs, the NEX-GDDP dataset has significantly improved the simulation ability of regional extreme precipitation in China, which is much closer to the observations, and the uncertainty is significantly smaller (Chen et al., 2017). Similar conclusions can be found in the simulation of extreme temperatures (Bao and Wen, 2017), which is therefore considered to be more suitable for simulating extreme weather at the city scale. A medium emission scenario (RCP4.5) was selected, which represents a scenario with government intervention (Hurt et al., 2011). With global efforts to reduce emissions, it is more likely to happen. Two periods were defined in the dataset, i.e., historical periods (1950–2005) and future periods (2006–2100). We chose 1950–2005 as the contemporary period and took the 15 years before and after the years reaching 2.0°C global warming as the future period, totaling 30 years. The arrival years for 2.0°C global warming were defined as the years in which the global average surface air temperature firstly increased to 2.0°C relative to the Industrial Revolution (1861–1880). The global average surface air temperature from 1860 to 1880 was calculated by the CMIP5 dataset (available online at <https://esgf-node.llnl.gov/search/cmip5/>). A total of 14 models out of 21 models were used in this study. The excluded 7 models are either with the arrival year of 2.0°C global warming beyond 2100 or not publicly available from CMIP5. See Supplementary data 1 for the models we used and the arrival years of 2.0°C global warming.

Indicators

Two indicators were selected to express the extreme heat and extreme precipitation, i.e., annual extreme heat days and daily maximum precipitation. An extreme heat day refers to a day during which the daily maximum temperature exceeds 35°C . Compared to other variables, these two indicators directly affect humans and are more easily understood by the public. Heat zones are defined as those areas in which the number of contemporary annual heat days is greater than four. And the extreme precipitation zones were defined as the areas with contemporary annual maximum daily precipitation greater than 80 mm.

Extreme climate analogs for each indicator

We used the multi-model median ensemble (MME) results of each indicator to calculate the extreme climate analogs. The MME results have been widely adopted in many studies to eliminate the bias due to some over-estimated or under-estimated climate models. For extreme climate indicators, especially for precipitation where uncertainty is higher in climate simulations, the performance of the MME results is better than that of individual models across China (Chen et al., 2017). After taking the MME result of each grid, we take the mean value of the urban areas to represent the climate state of a city. Then, the time series of historical periods and future periods of each city, i.e., two distributions, were generated for each city. We used the traversal method to find if any historical distribution of city i was identical to the given future distribution of the target city n . The two-sample Kolmogorov–Smirnov test (Massey, 1951) was used to decide if the two distributions were identical. The null hypothesis that the two distributions were identical would not be rejected when $p > 0.05$. On the premise of $p > 0.05$, the city with the smallest D value was selected as the best contemporary analog, which was expressed by eq.1. If all the historical distribution did not pass the test of $p > 0.05$, it was considered that the city was a novelty with a new extreme climate state. The novelty can be divided into two cases. One is a new extreme state that is beyond the contemporary extreme state, and the other is an intermediate state.

$$D_n = \max(F_n(x) - F_i(x)) \quad (1)$$

where $F_i(x)$ is the distribution of the contemporary periods of city i and $F_n(x)$ is the distribution of the future periods of city n .

Results and discussion

Changes in extreme heat days and precipitation

Fig. 2 shows the distributions of contemporary and future extreme heat days and precipitation in 369 cities, including the means and the variances. The distribution curves of the extreme heat days and daily maximum precipitation in the future would shift significantly to the right relative to that during contemporary times. That's, the means and the variances both increase, which represents a stronger extreme state in the future, and the higher probability of rare heat days or precipitation intensity in any year.

Extreme heat day changes more strongly. 308 of 369 cities exhibit increases in the mean under 2.0°C global warming, with an increase of 5.8 days on average and a maximum increase of 28.8 days. The variances for these cities increase by 1.7 days on average with a maximum increase of 4.2 days. As for extreme precipitation, all cities would experience increases in the means, which increased by 5.5 mm on average, with a maximum increase of 18.5 mm. Among them, 323 of 369 cities exhibit increases in the variances, with an average increase of 1.3 mm and a maximum increase of 6.7 mm.

Spatial distributions of the best analog to future cities

Extreme heat

Fig. 3 presents the distribution pattern of extreme heat days during contemporary times (background colors). Hebei Province (North China), Jiang Xi Province (East China), and Xinjiang Province (Northwest China) are the three heat zones in China, with 4.1 heat days per year on average. There are scattered heat areas surrounding Jiangxi and Hebei City Agglomeration, including the cities in Henan Province, Hubei Province, Hunan Province in Middle China, and Chongqing in Southwest China.

Contemporary analogs can be found for 241 of 369 cities under 2.0°C global warming. That is, there are 128 cities without contemporary analogs. Among them, 61 cities would have a new extreme heat state, which are mostly distributed in or around heat zones. And the

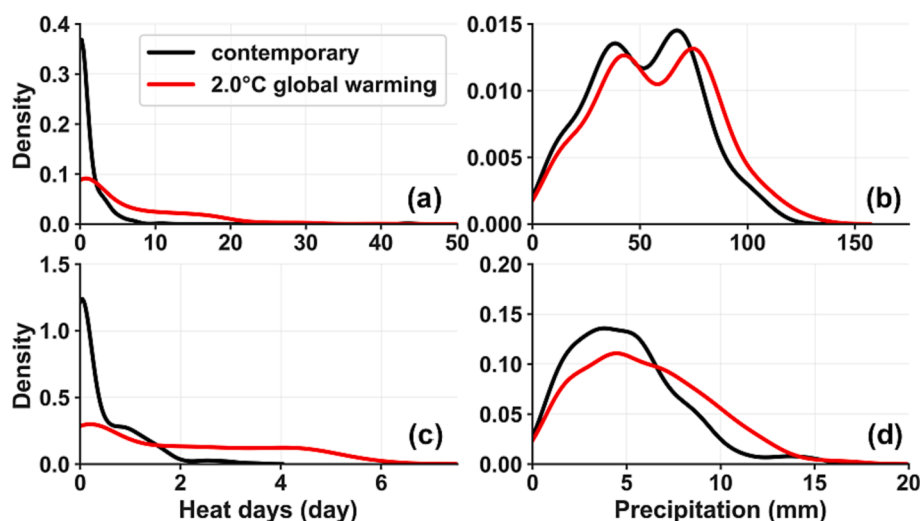


Fig. 2. Contemporary and future extreme heat and extreme precipitation distributions of all cities: (a) the means for annual heat days, (b) the means for annual maximum daily precipitation, (c) the variances for annual heat days, (d) the variances for annual maximum daily precipitation.

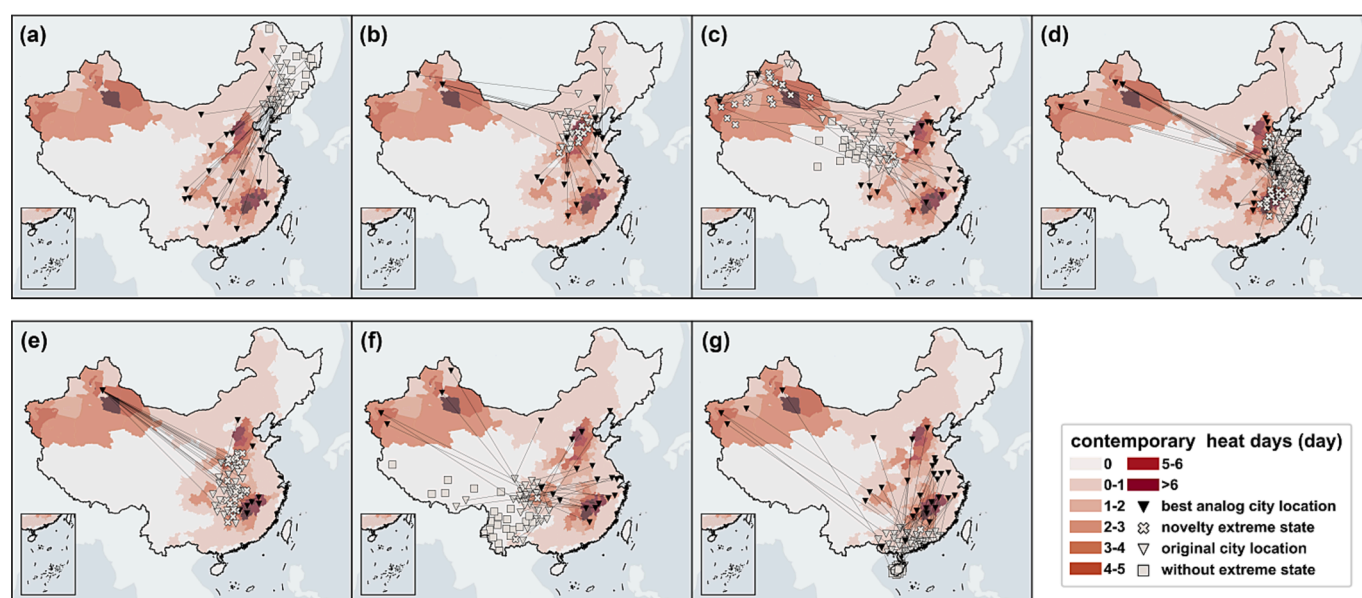


Fig. 3. Best extreme heat analogs map for cities under 2.0 °C global warming. (a) Northeast China, (b) North China, (c) Northwest China, (d) East China, (e) Middle China, (f) Southwest China, and (g) South China. Note: The background colors represent the contemporary average annual heat day distribution of each city.

cities in heat zones would all have higher frequencies that have not been seen in contemporary China. 67 cities would not experience extreme heat states. The cities that can avoid experiencing extreme heat states often have the following general characteristics: being located at high latitudes, high altitudes, or near coasts. Specifically, 90 % of the cities in the Tibetan Plateau would still avoid extreme heat states in the future due to their high altitudes. Meanwhile, 56 % of the cities in Hainan Province (South China) that are surrounded by the sea would also avoid extreme heat states.

For the 241 cities that can be matched, all of them are transitioning toward or around the three heat zones (Fig. 3), and 33 % of these cities would locate in the contemporary heat zones under 2.0 °C global warming. The cities surrounding heat zones would more readily transition to contemporary heat zones, e.g., Middle China, which is the most obvious region (Fig. 3e) with 84 % of its cities transitioning to heat zones. Followed by East China, 54 % of its cities transition to heat zones. Other regions are more likely to transition toward the edges of heat zones, such as Northeast China, North China, and South China (Fig. 3a,

b, g). Although their extreme heat states are weaker than that of the heat zones, significant increases still arise.

Extreme precipitation

As shown in Fig. 4, the contemporary extreme precipitation pattern in China can be roughly described as lower in the north and higher in the south, and the intensity of cities near the coasts is higher. This pattern shows an overall northeast-southwest trend. Jiangxi Province (East China) and the coastal areas of Guangdong and Hainan Province (South China) are the two extreme precipitation zones of China, with 88 mm of maximum daily precipitation on average.

Under 2.0 °C global warming, all cities are transitioning toward cities with higher extreme precipitation intensity (Fig. 4). Contemporary analogs can be found for the majority of cities (365 of 369 cities). Three cities in Hainan Province (South China) would experience record-breaking extreme precipitation states. A new intermediate state appeared for Hami, Xinjiang (Northwest China).

Approximate 64 % of northern cities would transition southward,

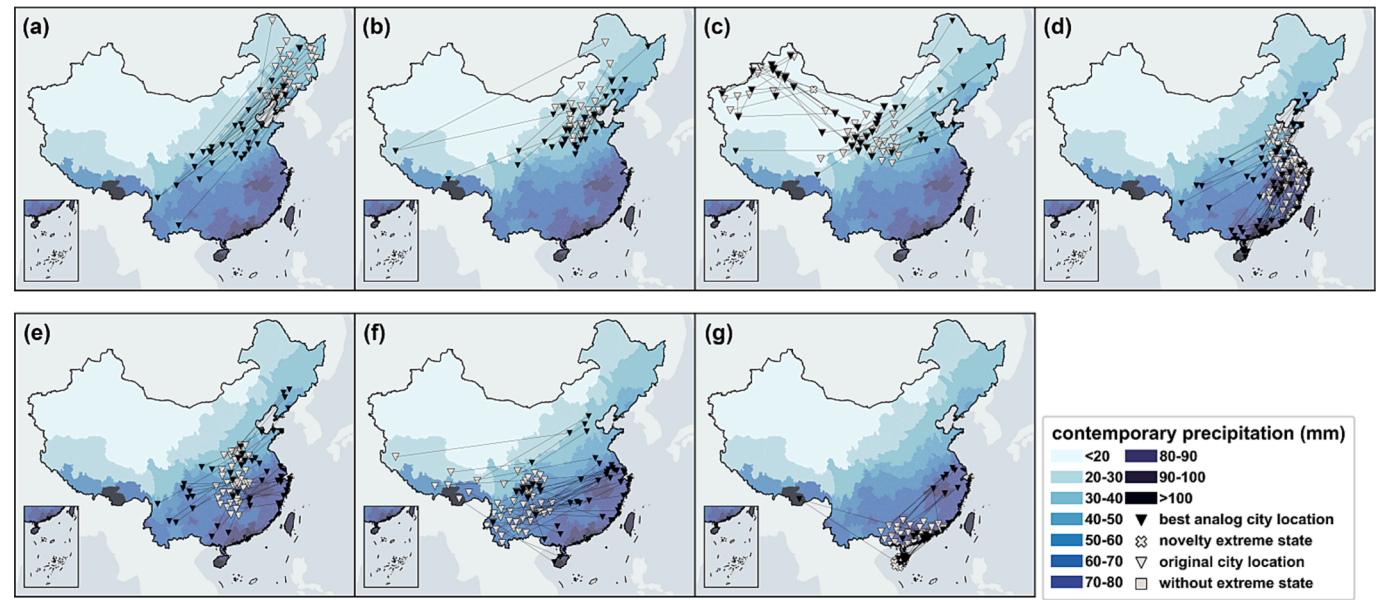


Fig. 4. Best extreme precipitation analogs map for cities under 2.0 °C global warming. (a) Northeast China, (b) North China, (c) Northwest China, (d) East China, (e) Middle China, (f) Southwest China, and (g) South China. Note: The background colors represent the contemporary average annual maximum precipitation distribution of each city.

with an average southward movement of 530 km (Fig. 4a-c), especially in Northeast China, which transitions 803 km southward (Fig. 4a). No obvious movement direction arises in Northwest China (Fig. 4c). Stronger increases can be seen in the southern cities. 21 % of the southern cities that are currently out of the extreme precipitation zones transition to extreme precipitation zones, which is mainly distributed in the areas around the extreme precipitation zones, i.e., South China (Fig. 4g) and East China (Fig. 4d). Approximate 64 % of the cities in South China are already located in extreme precipitation zones, and the proportion would reach 86 % under 2.0 °C global warming. At the same time, most cities in extreme precipitation zones also show increasing precipitation; therefore, the movement direction for South China is pointing toward another precipitation center (Jiangxi Province, East China), and the other direction is pointing toward Hainan (the stronger extreme precipitation zone in South China). For East China, 39 % of the cities that are currently outside of extreme precipitation zones transition to extreme precipitation zones in the future, and they significantly transition toward the southwest. For the other regions, few cities in Middle and Southwest China are transitioning toward extreme precipitation zones, but they are also transitioning toward areas with higher

extreme precipitation levels (Fig. 4e-f). Southwest China is transitioning eastward as a whole, while Middle China is spreading to all sides.

Contemporary analogs for super-large cities

We further focused on the changes in the super-large cities, as the extreme climate changes in super-large cities would have greater impacts than that in other cities. A total of 14 super-large cities with more than five million people are chosen as hot spots for analysis. Complete results are available in [Supplementary data 2](#).

These super-large cities would experience stronger extreme heat states (Table 1). Except for Harbin (Northeast China) and Qingdao (East China), which show no increases, the average increases in the means for the other 12 super-large cities are 1.4 times that of all cities. Among them, seven cities exhibit a greater increase in the means than that of all cities on average, including two megacities with populations larger than 10 million (i.e., Beijing and Tianjin, North China). The greatest increase in the mean would be as high as 16.05 days (Wuhan, Middle China), followed by 11.82 days (Shijiazhuang, North China). They would both experience new extreme heat states under 2.0 °C global warming, as well

Table 1
Means and variances of heat days in super-large cities and their contemporary analogs.

city	increase		future		Best analogy	Contemporary	
	mean	variance	Mean	variance		mean	variance
Wuhan	16.05	3.64	18.04	4.89	—		
Shijiazhuang	11.82	2.49	16.86	4.12	—		
Hangzhou	11.32	3.89	11.97	4.72	Wujiaqu	10.78	3.09
Chongqing	11.29	2.90	13.34	4.22	—		
Zhengzhou	9.10	3.24	11.54	4.19	Wujiaqu	10.78	3.09
Beijing	7.07	1.04	10.71	2.69	Wujiaqu	10.78	3.09
Tianjin	6.63	1.59	8.89	2.78	Wujiaqu	10.78	3.09
Guangzhou	4.16	2.38	4.18	2.45	Kashgar	3.81	1.82
Suzhou	3.00	2.19	3.00	2.19	Hengyang	3.24	2.05
Shanghai	1.47	1.35	1.47	1.35	Zhumadian	1.21	0.88
Chengdu	1.47	1.18	1.52	1.24	Jinhua	1.57	1.19
Shenzhen	0.39	0.62	0.39	0.62	Chuzhou	0.44	0.72
Qingdao	0.00	0.01	0.00	0.01	Foshan	0.01	0.03
Harbin	0.00	0.00	0.00	0.00	—		
All cities	4.83	1.43	5.74	1.86	—		

Note: the cities ordered by the increase in the means.

as Chongqing (Southwest China). Furthermore, we found that the top 6 increasing cities are all inland cities, while coastal cities would experience relatively small changes, such as Shanghai, Shenzhen, Qingdao. In terms of the variances, the cities with large increases in means are often accompanied by large variance changes, which indicate that the possibility of extreme heat events is higher.

Table 1 also lists the best contemporary analogs of super-large cities under 2.0 °C global warming, which would help these super-large cities to better understand and prepare for future extreme heat risks. For example, the future Beijing would become the contemporary Wujiaqu of Xinjiang (Northwest China).

Regarding the matching errors, it can be seen that the means and variances are close (Table 1), which fluctuate within [−20 %, 20 %] of the actual means and [−35 %, 16 %] of the actual variances. The errors may be amplified for cities with minor values, such as Qingdao.

For the extreme precipitation, super-large cities would also experience more extreme precipitation states. The average increase in the mean is 10 % higher than that of all cities, among which the southern cities are more prominent, with an average increase reaching 40 % higher than that of all cities. Eight cities have stronger increases in the means than that of all cities on average, with the highest increase in the mean as high as 10.32 mm (Suzhou), followed by 9.87 mm (Shanghai). In contrast to the changes in extreme heat states, these coastal cities face stronger extreme precipitation challenges, including Shanghai and Shenzhen in the south and Qingdao and Tianjin in the north. The super-large cities in the north would change less overall, but Zhengzhou (Middle China), as a northern city, appears to have a significant increase in the mean, which has outpaced Chongqing and Wuhan in the south. In terms of the variances, they exhibit the same patterns as those of extreme heat. The cities with high increases in the means also require attention to be paid to the higher probability of extreme events.

The best contemporary analogs of super-large cities under 2.0 °C global warming are shown in Table 2. The errors in the means are very small and fluctuate within [−2.7 %, 1.6 %] of the actual means and [−31 %, 27 %] of the actual variance values. Furthermore, we found that 86 % of the contemporary analogs have smaller variances, which indicates that the possibility of extreme events in the future would exceed that during contemporary times.

Uncertainties

The sources of uncertainty can be divided into the following aspects: selection of indicators, selection of periods, selection of matching methods, and climate models. According to existing studies (Grenier et al., 2013), what matters most is the differences between climate

models. Here, the multi-model increases in the means, and the variances are shown in Fig. 5. The results show that all models support positive changes (i.e., increases) in the means and the variances of heat days. The MME results generally indicate that the median levels of changes in the means, but the variances are lower than that of every single model, which indicates that the probability of extreme events in these cities would be higher than we expected. The MME results avoid extreme errors, but they also reduce the variability as well.

For extreme precipitation, all models support the positive changes in the mean, but there are some differences in the variance changes. Among them, 8 models (14 in total) support the increases in the variances. Again, the MME results generally indicate the median levels of changes in the means and exhibits positive variance changes after the integration of all models, located in ~ 60 quantiles.

Due to the large differences among climate models, different matching results will be generated for a specific city when using different model data in this work. Our results emphasize the results that are based on the MME results, which can reflect the median level in the mean state.

Limitations

Describing extreme climate analogs is only the first step, and factors such as the level of city development are not considered, while these factors are also critical for further describing city vulnerabilities and risk assessments (Ford et al., 2010; Horváth, 2008). The differences of economic development level and natural conditions would affect whether city managers can implement the adaptation measures. Quantifying these differences is complex and could be studied further in the future. Moreover, two simple indicators are chosen to express the basic extreme heat and precipitation changes. More extreme climate indicators, both single and multivariate indicators can be further analyzed in future study, such as the night temperature related to human health and maximum accumulated 5-day precipitation related to flood risk, extreme winds and compound dry and heat events.

As for the climate model data, we use the MME results to reduce the bias among different climate models. The effect of model bias needs to be further studied in the future, as it has an impact on the shape of extreme value distribution. For cities with large model uncertainties, more policies to deal with uncertainties need to be considered. Also, considering the limited ability of a global dataset to capture the extreme event at the city scale, more precise regional climate models are needed in the future.

Some additional city characteristics, such as the urban heat island effect and stronger convection effects, may underestimate temperature

Table 2
Means and variances of RX1D in large cities and their contemporary analogs.

city	increase		future		Best analogy	Contemporary	
	mean	variance	mean	variance		mean	variance
Suzhou	10.32	1.93	85.95	9.82	Zhongshan	86.36	9.45
Shanghai	9.87	3.66	84.50	11.30	Shantou	84.75	10.17
Shenzhen	9.79	3.06	108.03	12.00	Sanya	109.78	15.25
Guangzhou	7.82	1.43	90.20	10.69	Dingan	90.97	10.66
Chengdu	7.10	3.13	65.60	8.73	Zhuzhou	64.80	6.37
Zhengzhou	6.24	1.33	47.17	4.92	Ankang	47.13	4.79
Hangzhou	6.14	0.47	78.94	8.09	Guigang	79.22	8.08
Chongqing	4.88	1.80	64.37	6.12	Loudi	63.60	5.62
Qingdao	4.06	0.17	49.05	3.68	Xuzhou	49.02	3.65
Tianjin	4.02	1.17	41.21	4.79	Zhengzhou	40.93	3.59
Wuhan	3.97	2.28	66.68	8.02	Xi'an	64.87	5.53
Harbin	3.91	0.78	37.88	3.06	Ali	37.86	2.78
Beijing	3.71	−0.70	38.71	2.96	Fuxin	38.74	2.81
Shijiazhuang	3.37	0.64	38.33	3.63	Jiaozuo	38.21	3.46
All cities	5.45	1.04	57.55	5.93	—		

Note 1: RX1D refers to the annual maximum daily precipitation.

Note 2: the cities are ordered by the increases in the means.

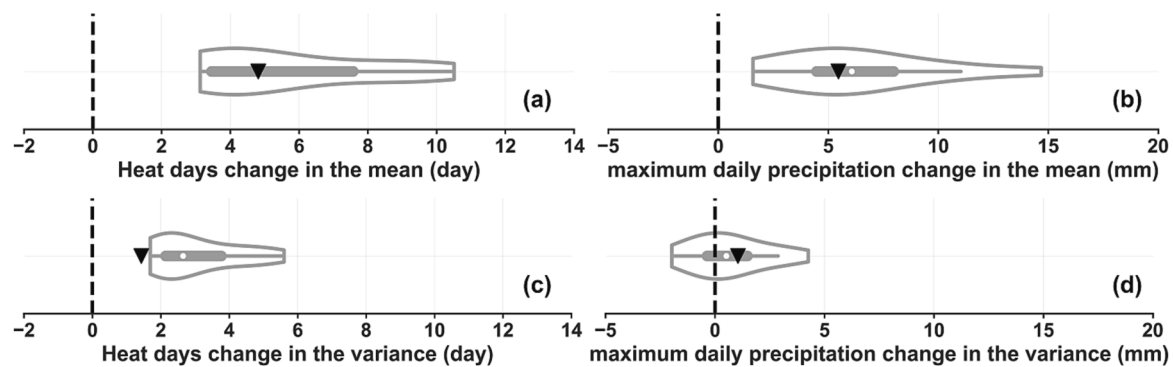


Fig. 5. Violin plots of the multi-model changes in the means and the variances: (a) changes in the means of extreme heat days, (b) changes in the means of extreme precipitation, (c) changes in the variances of extreme heat days, and (d) changes in the variances of extreme precipitation. Black triangles: multi-model median ensemble.

and extreme precipitation, especially in large cities (Gu and Li, 2018; McCarthy et al., 2010; Zhao et al., 2014). It is considered by keeping the temperature and precipitation spatial pattern and magnitude observed in historical data though the bias correction (Thrasher et al. 2012), and is roughly reflected in our results. However, the increasing population and emissions in the future, especially in large cities, would significantly affect the urban heat island effect and stronger convection effects, which can be considered in the future study. With the refinement of climate model data, these uncertainties are expected to decrease (Lawrence et al., 2016).

Conclusion

Frequent extreme weather caused by climate change affects the normal operation and safety of cities, and the public and city managers need a clearer understanding of the changes and impacts to participate in adaptation actions. In this study, we first analyzed the extreme heat and extreme precipitation changes for 369 cities in mainland China and their contemporary analogs under 2.0 °C global warming. We found that 83 % of cities would face increases in both the means and variances of extreme heat, and 100 % of cities would face increases in both the means and variances of extreme precipitation. Climate-analogy map was used to help the public and city managers find a similar city to learn experience to adapt to climate extremes. Compared with previous studies, we pay attention to extreme variables separately and guarantee a higher matching rate, which can improve the utility of climate-analog mapping. For extreme heat, 17 % of cities would experience a new state that is not shown in contemporary cities, and 65 % of cities are transitioning to hotter places. The remaining 18 % of cities, which are mostly located at high altitudes or high latitudes, could still avoid extreme heat states. For extreme precipitation, we find the best analogs for 99 % of cities, and they are transitioning to locations with higher extreme precipitation levels. On the whole, the cities with extreme states today would approach even more extreme states in the future, such as those in middle China and southeast China. As representatives of regions with contemporary extreme heat and extreme precipitation, the future increases in the means would still be 2.7 times and 1.7 times higher than other regions, respectively.

The increases in the means and variances of the extreme heat and extreme precipitation states imply more frequent heat weather and stronger precipitation intensities in the future, as well as higher probabilities of catastrophic extreme events. For most cities, extreme climate changes would present challenges, especially for super-large cities, with 10 %-40 % stronger than the average of all cities. As an easy-to-understand quantitative climate change output tool, this analysis can provide the public with a more intuitive understanding of extreme city climate changes and provide a clearer reference for city extreme climate managers in subsectors from similar cities.

CRediT authorship contribution statement

Qianzhi Wang: Methodology, Formal analysis, Conceptualization, Writing – original draft. **Kai Liu:** Conceptualization, Writing – review & editing. **Xiaoyong Ni:** Writing – review & editing. **Ming Wang:** Writing – review & editing.

Declaration of Competing Interest

The authors declare that they have no known competing financial interests or personal relationships that could have appeared to influence the work reported in this paper.

Data availability

Data will be made available on request.

Acknowledgements

This work was supported by the Major Program of National Natural Science Foundation of China (No. 72091512). The financial support is highly appreciated.

Climate scenarios used were from the NEX-GDDP dataset, prepared by the Climate Analytics Group and NASA Ames Research Center using the NASA Earth Exchange, and distributed by the NASA Center for Climate Simulation (NCCS). The data support is highly appreciated.

Appendix A. Supplementary data

Supplementary data to this article can be found online at <https://doi.org/10.1016/j.cliser.2023.100348>.

References

- Axios, 2022. Heat wave kills more than 2,000 people in Spain and Portugal. (available at: <https://www.axios.com/2022/07/18/heat-wave-europe-death-toll>) (Accessed 13 August 2022).
- Bao, Y., Wen, X.Y., 2017. Projection of China's near- and long-term climate in a new high-resolution daily downscaled dataset NEX-GDDP. *J. Meteorolog. Res.* 31, 236–249.
- Bastin, J.F., Clark, E., Elliott, T., Hart, S., van den Hoogen, J., Hordijk, I., Ma, H., Majumder, S., Manoli, G., Maschler, J., 2019. Understanding climate change from a global analysis of city analogues. *PLoS One* 14, e0217592.
- Bell, J.E., Brown, C.L., Conlon, K., Herring, S., Kunkel, K.E., Lawrimore, J., Luber, G., Schreck, C., Smith, A., Uejio, C., 2018. Changes in extreme events and the potential impacts on human health. *J. Air Waste Manag. Assoc.* 68, 265–287.
- Byers, E., Gidden, M., Leclère, D., Balkovic, J., Burek, P., Ebi, K., Greve, P., Grey, D., Havlik, P., Hillers, A., 2018. Global exposure and vulnerability to multi-sector development and climate change hotspots. *Environ. Res. Lett.* 13, 055012.
- Carter, J.G., Cavan, G., Connelly, A., Guy, S., Handley, J., Kazmierczak, A., 2015. Climate change and the city: Building capacity for urban adaptation. *Prog. Plan.* 95, 1–66.
- Casto, C.A., 2014. Crisis management: a qualitative study of extreme event leadership. *Management. Kennesaw State University*, p. 626.

- Chan, F.K.S., Griffiths, J.A., Higgitt, D., Xu, S., Zhu, F., Tang, Y.-T., Xu, Y., Thorne, C.R., 2018. "Sponge City" in China—a breakthrough of planning and flood risk management in the urban context. *Land Use Policy* 76, 772–778.
- Chen, H.P., Sun, J.Q., Li, H.X., 2017. Future changes in precipitation extremes over China using the NEX-GDDP high-resolution daily downscaled data-set. *Atmos. Oceanic Sci. Lett.* 10, 403–410.
- Cheung, W., Feldman, D., 2019. Can citizen science promote flood risk communication? *Water* 11, 1961.
- China State Council, 2014. Circular of The State Council on adjusting the standards for the classification of city sizes (In Chinese). (available at: http://www.gov.cn/gongbao/content/2014/content_2779012.htm) (Accessed 9 April 2022).
- Dodman, D., Hayward, B., Pelling, M., Broto, V.C., Chow, W., Chu, E., Dawson, R., Khirfan, L., McPhearson, T., Zheng, Y., Ziervogel, G., 2022. Cities, Settlements and Key Infrastructure. *Climate Change 2022: Impacts, Adaptation, and Vulnerability. Contribution of Working Group II to the Sixth Assessment Report of the Intergovernmental Panel on Climate Change*. Cambridge University Press.
- European Space Agency, 2020. Land Cover Map 2019. (available at: <http://maps.elie.ucl.ac.be/CCI/viewer/>) (Accessed 1 December 2020).
- Fitzpatrick, M.C., Dunn, R.R., 2019. Contemporary climatic analogs for 540 North American urban areas in the late 21st century. *Nat. Commun.* 10, 1–7.
- Ford, J.D., Kesikitalo, E., Smith, T., Pearce, T., Berrang-Ford, L., Duerden, F., Smit, B., 2010. Case study and analogue methodologies in climate change vulnerability research. *Wiley Interdiscip. Rev. Clim. Chang.* 1, 374–392.
- Gao, J., Sun, Y., Liu, Q., Zhou, M., Lu, Y., Li, L., 2015. Impact of extreme high temperature on mortality and regional level definition of heat wave: a multi-city study in China. *Sci. Total Environ.* 505, 535–544.
- Glantz, M.H., 2019. Societal responses to regional climatic change: forecasting by analogy. Routledge.
- Greene, S., Kalkstein, L.S., Mills, D.M., Samenow, J., 2011. An examination of climate change on extreme heat events and climate–mortality relationships in large US cities. *Weather Clim. Soc.* 3, 281–292.
- Grenier, P., Parent, A.-C., Huard, D., Anctil, F., Chaumont, D., 2013. An assessment of six dissimilarity metrics for climate analogs. *J. Appl. Meteorol. Climatol.* 52, 733–752.
- Gu, Y., Li, D., 2018. A modeling study of the sensitivity of urban heat islands to precipitation at climate scales. *Urban Clim.* 24, 982–993.
- Guerreiro, S.B., Dawson, R.J., Kilsby, C., Lewis, E., Ford, A., 2018. Future heat-waves, droughts and floods in 571 European cities. *Environ. Res. Lett.* 13, 034009.
- Hallegatte, S., Hourcade, J.-C., Ambrosi, P., 2007. Using climate analogues for assessing climate change economic impacts in urban areas. *Clim. Change* 82, 47–60.
- Horváth, L., 2008. Use of Spatial Analogy in Analysis and Valuation of Climate Scenarios. Corvinus University of Budapest. Doctoral Dissertation.
- Hurt, G.C., Chini, L.P., Frolking, S., Betts, R., Feddema, J., Fischer, G., Fisk, J., Hibbard, K., Houghton, R., Janetos, A., 2011. Harmonization of land-use scenarios for the period 1500–2100: 600 years of global gridded annual land-use transitions, wood harvest, and resulting secondary lands. *Clim. Change* 109, 117–161.
- Jiang, Y., Zevenbergen, C., Ma, Y., 2018. Urban pluvial flooding and stormwater management: A contemporary review of China's challenges and "sponge cities" strategy. *Environ Sci Policy* 80, 132–143.
- Kopf, S., Ha-Duong, M., Hallegatte, S., 2008. Using maps of city analogues to display and interpret climate change scenarios and their uncertainty. *Nat. Hazards Earth Syst. Sci.* 8, 905–918.
- Lawrence, D.M., Hurt, G.C., Arneth, A., Brovkin, V., Calvin, K.V., Jones, A.D., Jones, C. D., Lawrence, P.J., Noblet-Ducoudré, N.D., Pongratz, J., 2016. The Land Use Model Intercomparison Project (LUMIP) contribution to CMIP6: rationale and experimental design. *Geosci. Model Dev.* 9, 2973–2998.
- Liu, Z., Cheng, W., Jim, C.Y., Morakinyo, T.E., Shi, Y., Ng, E., 2021. Heat mitigation benefits of urban green and blue infrastructures: A systematic review of modeling techniques, validation and scenario simulation in ENVI-met V4. *Build. Environ.* 200, 107939.
- Mahony, C.R., Cannon, A.J., Wang, T., Aitken, S.N., 2017. A closer look at novel climates: new methods and insights at continental to landscape scales. *Glob. Chang. Biol.* 23, 3934–3955.
- Massey Jr, F.J., 1951. The Kolmogorov-Smirnov test for goodness of fit. *J. Am. Stat. Assoc.* 46, 68–78.
- Maurer, E.P., Hidalgo, H.G., 2008. Utility of daily vs. monthly large-scale climate data: an intercomparison of two statistical downscaling methods. *Hydrol. Earth Syst. Sci.* 12, 551–563.
- McCarthy, M.P., Best, M.J., Betts, R.A., 2010. Climate change in cities due to global warming and urban effects. *Geophys. Res. Letters* 37.
- Murawski, S., 1993. Climate change and marine fish distributions: forecasting from historical analogy. *Trans. Am. Fish. Soc.* 122, 647–658.
- People's Government of Henan, 2021. 10th press conference of Henan flood control and disaster relief. (available at: <http://www.henan.gov.cn/2021/08-02/2194036.html>) (Accessed 2 August 2021).
- Sanderson, M., Hanlon, H., Palin, E., Quinn, A., Clark, R., 2016. Analogues for the railway network of Great Britain. *Meteorol. Appl.* 23, 731–741.
- Seneviratne, S.I., Zhang, X., Adnan, M., Badi, W., Dereczynski, C., Luca, A.D., Ghosh, S., Iskandar, I., Kossin, J., Lewis, S., Otto, F., Pinto, I., Satoh, M., Vicente-Serrano, S.M., Wehner, M., Zhou, B., 2021. Weather and Climate Extreme Events in a Changing Climate. *Climate Change 2021: The Physical Science Basis. Contribution of Working Group I to the Sixth Assessment Report of the Intergovernmental Panel on Climate Change*. Cambridge University Press, Cambridge, United Kingdom and New York, NY, USA, pp. 1513–1766. <https://doi.org/10.1017/9781009157896.013>.
- Shen, G., Hwang, N.H., 2019. Spatial-temporal snapshots of global natural disaster impacts Revealed from EM-DAT for 1900–2015. *Geomat. Nat. Haz. Risk* 10, 912–934.
- Szenteleki, K., Horváth, L., Ladányi, M., 2012. Climate risk and climate analogies in Hungarian viticulture. *Int. Conf. Futur. Environ. Energy* 250–254.
- Thrasher, B., Maurer, E.P., McKellar, C., Duffy, P.B., 2012. Technical Note: Bias correcting climate model simulated daily temperature extremes with quantile mapping. *Hydrol. Earth Syst. Sci.* 16 (9), 3309–3314.
- U.N. Population Division, 2018. The World's cities in 2018: data booklet 2018. United Nations, New York.
- Vaidya, H., Chatterji, T., 2020. SDG 11 Sustainable Cities and Communities, Actioning the Global Goals for Local Impact. Springer 173–185.
- Webb, L., Watterson, I., Bhend, J., Whetton, P., Barlow, E., 2013. Global climate analogues for winegrowing regions in future periods: projections of temperature and precipitation. *Aust. J. Grape Wine Res.* 19, 331–341.
- Wood, A.W., Maurer, E.P., Kumar, A., Lettenmaier, D.P., 2002. Long-range experimental hydrologic forecasting for the eastern United States. *J. Geophysical Research-Atmospheres* 107, 4429.
- Wood, A.W., Leung, L.R., Sridhar, V., Lettenmaier, D.P., 2004. Hydrologic implications of dynamical and statistical approaches to downscaling climate model outputs. *Clim. Change* 15, 189–216.
- Zhao, L., Lee, X., Smith, R.B., Oleson, K., 2014. Strong contributions of local background climate to urban heat islands. *Nature* 511, 216–219.